Kogaku Zassi, **91**, 723 (1970).
(14) M. Aizawa, J. Mizuguchi, S. Suzuki, S. Hayashi, T. Suzuki, N. Mitomo and H. Toyama, *Bull. Chem. Soc., Japan*, **45**, 3031 (1962).
(15) H. B. Lee, M. S. Jhon, and J. D. Andrade, *J. Colloid Interface Sci.*, **51**, 225 (1975).
(16) D. E. Gregonis, G. A. Russel and J. D. Andrade, *Polymer*, **19**, 1279 (1978).
(17) D. E. Gregonis, C. M. Chen, and J. D. Andrade. in J. D. Andrade, Ed., "Hydrogels for Medical and Related Applications", ACS Symposium Series 31, Amer. Chem. Soc., Washington, D. C., (1976), p. 88.
(18) N. Bekkedahl, J. Research of the National Bureau of Standards, **42**, 145 (1949).
(19) M. Aizawa and S. Suzuki, *Bull. Chem. Soc. Japan*, **44**, 2967 (1971).
(20) R. C. West, Ed., "Handbook of Chemistry and Physics", 59th Ed., CRC Press, Inc., 1979.
(21) D. P. Shoemaker and C. W. Garland, "Experiments in Physical Chemistry", 2nd Ed., P. 194, McGraw-Hill Kogakusha, 1967.
(22) H. P. Schwan, in W. L. Nastuk Ed., "Physical Techniques in Biological Reserach", Vol. VI, p. 337, Academic Press., 1963.
(23) E. A. Moelwyn-Hughes, "Physical Chemistry", p. 464 and 748, Pergamon Press, London, 1961.
(24) S. Glasstone, K. J. Laidler, and H. Eyring, "The Theory of Rate Processes", McGraw-Hill Book C. Inc., New York, 1941.
(25) S. H. Choi, M. S. Jhon, and J. D. Andrade, *J. Colloid and Interface Sci.*, **61**, 1 (1977).
(26) G. A. Russel, P. A. Hiltner, D. E. Gergonis, A. C. de Visser and J. D. Andrade, *J. Polym. Sci. Polym. Phys. Ed.*, **18**, 1271 (1980).

Theoretical Study of the Effects of Cation on *t*RNA

Kwang Oh Koh and Mu Shik Jhon

Department of Chemistry, Korea Advanced Institute of Science and Technology, P. O. Box 150 Chongyangni, Seoul 131, Korea, 1981 *(Received February 20, 1981)*

The effects of cation on *t*RNA have been theoretically investigated using the semiempirical potential enregy functions. The binding of Mg^{2+} to the model compound and the hydration scheme of the anticodon loop have been determined, and their stabilization energies produced by the introduction of magnesium pentahydrate and water molecules in the first hydration shell were calculated. The results indicate that magnesium pentahydrate is important for decreasing the flexibility of the anticodon loop and satisfying the large Y37 stereochemically during the protein synthesis. The effects of Mg^{2+} on the hydration scheme were also investigated.

Introduction

Cation is essential for many biological reactions. Especially, Mg^{2+} is important for the protein synthesis. Therefore much efforts, both theoretical and experimental, have gone into the study of cation binding to nucleic acids and components[1-5]

Recently, three dimensional structure of yeast phenylalanine *t*RNA(*t*RNA^{phe}) have been determined by X-ray crystallographic studies[6-8]. The ordered yeast *t*RNA^{phe} lattice has made possible the elucidation of the structure of this molecule in both orthorhombic and monoclinic crystal forms. These studies indicate the existence of at least four site-specifically bound hydrated Mg^{2+} ions in orthorhombic crystal of yeast *t*RNA^{phe}.

And very recently, Kim and Jhon[9] have calculated the hydration scheme of *t*RNA and stabilization energy due to the presence of water molecules in orthorhombic crystal of yeast *t*RNA^{phe} without considering Mg^{2+}.

Therefore it is important and more realistic that since Mg^{2+} is present in the anticodon loop, we consider the effects of Mg^{2+} on the stabilization and hydration of the anticodon loop.

In this study, using the semiempirical potential energy functions, it is found that Mg^{2+} in the anticodon loop is important for the conformation of P37, and the stabilization energy of Mg^{2+} is greater than that of the water molecules in the hydration shell.

The Method

The methods for the optimization of the Mg^{2+} cation binding, its hydration scheme, and the stabilization energy due to the hydration follow the general formula presented by Perahia *et al*[10]. The interaction energies have been obtained by using the potential energy functions by Caillet and Claverie[11,12] that are composed of three long-range contributions (electrostatic, polarization and dispersion) and a short range repulsive term. The nature of energy functions and their parameters are discussed elsewhere[9-12].

Electrostatic Energy. The net atomic charges of the model compound are taken from Renugopalakrishnan *et al*[13]. and those of the ϕ base of the anticodon loop have been calculated using the Del Re method[14] for σ charge and the Hückel method for π charge. It is assumed that the dielectric constant of this system is unity and the net charge of Mg^{2+} is to be +2.

Polarization Energy. Polarization energy is evaluated as the sum of atom polarization contributions. And the experimental value[15] is used for Mg^{2+}.

Dispersion and Respulsion Energies. The modified Kitaigorodskii formula is used to obtain the dispersion and repulsion energy contributions. The Van der Waals radius of Mg^{2+} is taken from Stokes.[16].

The modification of the repulsion term due to the atomic electron population for Mg^{2+} is neglected. The parameter, $k_{Mg^{2+}}$ is obtained as 5.9 from the hydration energy[17] of Mg^{2+}.

The Case of the Hydrogen Bond. Because the charge-transfer contribution becomes significant for the hydrogen bond, the parameters contained in the formulas are somewhat modified according to the extent of the hydrogen bond strength.

The Model Compound

Of the 76 nucleotides of yeast $tRNA^{phe}$, we have considered 29 to 40 nucleotides as a model compound because the effects on Mg^{2+} is negligible beyond the model compound. The model compound consists of twelve nucleotides, A(29), G(30), A(31), C_m(32), U(33), G_m(34), A(35), A(36), Y(37), A(38), ϕ(39) and C_m(40) in sequence from 5'-side; The subscript m denotes that 2'-hydroxyl group of this nucleotide is methylated and the number in parenthesis represents the order of the nucleotides from 5'-end in the whole $tRNA^{phe}$ sequence. Here, Y is an alkylated purine nucleotide and ϕ is an pseudouridine.

The atomic coordinates of the model compound have been obtained from the crystal structure in orthorhombic form[18]. And we have chosen a dihedral angle of 222° for the orientation of H[Oϕ_2''].

Determination of the Hydration Scheme of the Anticodon Loop and Evaluation of the Stabilization Energy due to Mg^{2+} and the Hydration

The optimum position of Mg^{2+} bound to model compound was determined by the known coordinates of three successive atoms, a distance between Mg^{2+} and one anion of phosphate group and their dihedral angle. The geometrical position of water molecule with respect to the model compound is described with six parameters d,$\theta1$,$\theta2$,$\varphi1$,$\varphi2$ and $\varphi3$ dipicted in Figure 1. If A1, A2 and A3 are three successive atoms on the model compound with known coordinates and with A1 forming a hydrogen bond with the water molecule, d is the A1H distance, $\theta1$ and $\theta2$ are A2A1H and A1HO angles, respectively, and $\varphi1$, $\varphi2$ and $\varphi3$ correspond to dihedral angles around A2A1, A1H and HO, respectively.

The cartesian coordinates of Mg^{2+} and the water molecule can be obtained by the computational method developed by Thompson[19] with these parameters. The probable hydration scheme has been established successively for each water molecule until no more water molecule can be located by a direct binding to the model compound. And the locations of Mg^{2+} and the hydrated water molecules have been optimized by minimizing the interaction energy of each water molecule with the variation of parameters simultaneously using a minimization method suggested by Fletcher[20].

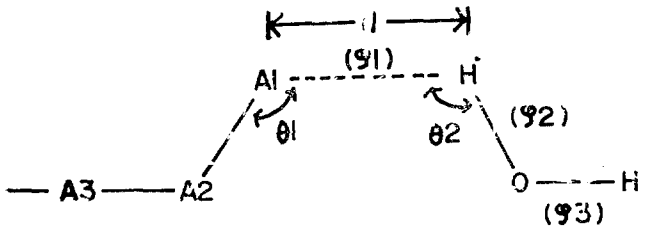

Figure 1. Variables defining the position of a water molecule with respect to the atoms of attachment.

The stabilization energy due to Mg^{2+} and the hydration has been calculated by comparing the internal interaction energies between the different groups of the essential subunits of the model compound. The hydrated model compound with Mg^{2+} is considered as a supermolecule, a unique entity formed by the substrate, Mg^{2+} and water molecules in the first hydration shell. The water molecules involved in two or three hydrogen bonds were counted with the subunit to which the binding was the strongest.

Results and Discussion

Binding of Mg^{2+} to the Model Compound

In an aqueous environment, Mg^{2+} ion exists as a hexa-hydrated form, $[Mg(H_2O)_6]^{2+}$. But hexa-hydrated form cannot enter to the anticodon loop because of the size of the anticodon loop. It has been found that Mg^{2+} in the anticodon loop is bound to five water molecules in octahedral coordination by X-ray crystallographic result[6]. According to this result, Mg^{2+} directly coordinates to oxygen atom of P37 instead of the removed water molecule. Thus, Mg^{2+} has been considered in octahedral coordination and the location of $[Mg(H_2O)_5]^{2+}$ optimized to the technique mentioned previously.

The determined location of $[Mg(H_2O)_5]^{2+}$ is projected in Figure 2. And the optimized distances of Mg^{2+} and oxygen atoms(from either water molecule or phosphate) and optimum positions are listed in Tables 1 and 2. The optimum average coordination distances are 2.03 Å between Mg^{2+} and oxygen (from either water molecule or phosphate), 4.1 Å between Mg^{2+} and oxygen which is hydrogen bonded to the water molecules in $[Mg(H_2O)_5]^{2+}$, and in good agreement with the average Mg^{2+}-oxygen lengths observed in crystals[6].

The average interaction energies between Mg^{2+} and its coordinated water molecules are −65.4 kcal/mole (see Table 3), and in good agreement with ab initio results[17].

The interaction energy between only five water molecules bound to Mg^{2+} and anticodon loop is 15 kcal/mole. Thus these five water molecules destabilize the anticodon loop.

TABLE 2: Optimum Positions of $[Mg(H_2O)_5]^{2+}$

Mg^{2+}	Optimum positions			Reference atoms			Binding energies
	d	θ	φ	A1	A2	A3	(kcal/mole)
	2.06	165	313	02(P37)	P37	O5′(P37)	−1392

Water	Optimum positions						Reference atoms			Binding energy
	d	$\theta1$	$\varphi1$	$\theta2$	$\varphi2$	$\varphi3$	A1	A2	A3	(kcal/mole)
H_2O (C32 02)	1.51	101	161	191	219	288	O2(C32)	C2(32)	N1(C32)	−39.3
H_2O (P37 05′)	3.39	107	27	350	142	334	O2(P37)	P37	O5′(P37)	−17.2
H_2O (Y37 N7)	1.88	96	165	190	350	180	N7(Y37)	C8(Y37)	N9(Y37)	−33.7
H_2O (ϕ39 02)	1.99	122	158	150	290	120	O2(39)	C2(39)	N3(39)	−63.2
H_2O (Mg^{2+})	3.85	148	20	230	340	270	O2(P37)	P37	O5′(P37)	−41.3

Atoms which are bonded to H_2O are in parentheses.

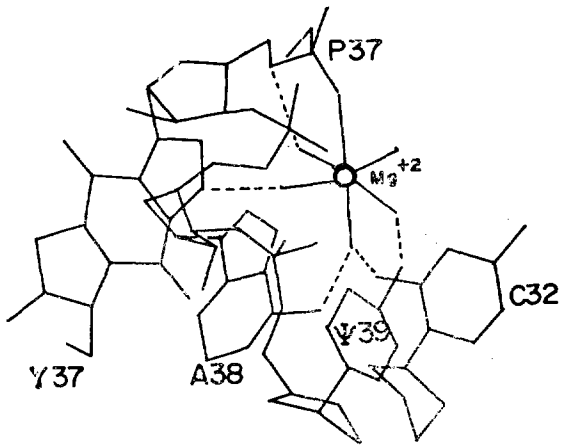

Figure 2. Binding of $[Mg(H_2O)_5]^{2+}$.

TABLE 1: Optimized Distances of Mg^{2+} and Water Molecules

	d(Å)	d(H-bond)
Mg^{2+}...(O(H_2O)	1.96	1.51(C32 O2) 1.64(A38 N6H)
Mg^{2+}···O(P37 O2P)	2.06	—
Mg^{2+}···O(H_2O)	2.13	1.73(P37 O5′)
Mg^{2+}···O(H_2O)	2.07	1.88(Y37 N7)
Mg^{2+}···O(H_2O)	2.08	1.99(ϕ39 O2)
Mg^{2+}···O(H_2O)	1.91	—
Average	2.03	
Exp	2	

Atoms which are hydrogen bonded to H_2O are in parentheses.

But these five water molecules are not removed from Mg^{2+} because of large interaction energy (−65.4kcal/mole) with Mg^{2+}.

In Table 4, the site energy of Mg^{2+} is listed. As seen in the table, in case there is only Mg^{2+}, Mg^{2+} at the *B* site of P37 group more stabilizes model compound than that at the *E* site. According to Pullman's result[19], $[Mg(H_2O)_5]$ is more stable at the E site than at *B* site.

The effects of $[Mg(H_2O)_5]^{2+}$ at the *E* site on the anticodon loop are as follows. First, magnesium pentahydrate at the *E* site stabilizes the whole anticodon loop, but that at the *B* site stabilizes mainly P37 group. Thus magnesium pentahydrate decreases the flexibility of the antidocon loop so that *t*RNA interacts with *m*RNA easily during the protein synthesis. Second, magnesium pentahydrate at the *E*

TABLE 3: Interaction Energies of Mg^{2+} and Substrate (in kcal/mole)

	E_{el}	E_{pol}	E_{dsp}	E_{rep}	E_{tot}
Mg^{2+} ($5H_2O$)	−1153	−404	−68	21	−1392
Mg^{2+}	−929	−153	−12	29	−1065
	ΔE=−327(−65.4/H_2O)				
ab initio	ΔE=−298(−59.6/H_2O)				

TABLE 4: Site Energies of Mg^{2+}(kcal/mole)

Site	E_{el}	E_{Pol}	E_{dsp}	E_{rep}	E_{tot}
E	−929	−153	−12	29	−1065
B	−915	−249	−34	76	−1122

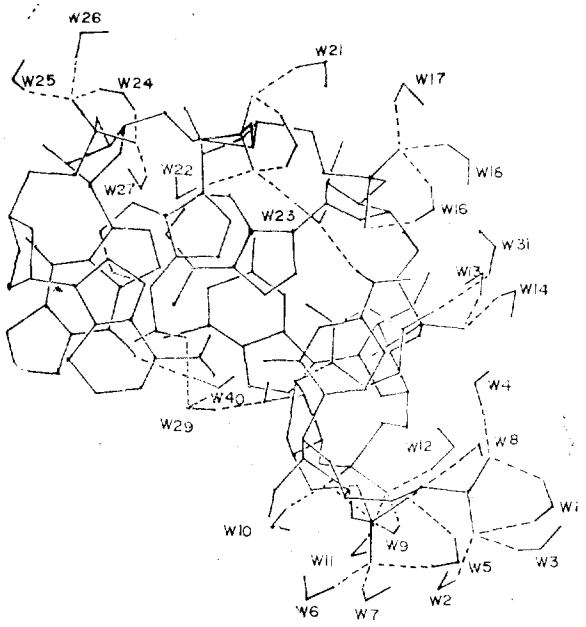

Figure 3. Hydration of the anticodon loop.

TABLE 5: Optimum Locations and the Interaction Energies of the Hydrated Water Molecules in the Anticodon Loop of *t*RNA

Water	Optimum positions						Reference atoms			Binding
	d (A)	$\theta 1$ (deg)	$\varphi 1$ (deg)	$\theta 2$ (deg)	$\varphi 2$ (deg)	$\varphi 3$ (deg)	A1	A2	A3	energies (kcal/mole)
W1	1.80	102	129	144	16	323	01(p32)	P32	05'(P32)	−25.7
W2	1.69	118	299	138	300	355	01(P32)	P32	05'(P32)	−17.7
W3	1.78	116	206	151	301	345	01(P32)	P32	05'(P32)	−19.3
W4	1.63	124	87	155	320	147	02(P32)	P32	05'(P32)	−19.1
W5	1.87	102	122	147	25	336	01(P33)	P33	O5'(P33)	−26.0
W6	1.72	134	307	139	313	3	01(P33)	P33	05'(P33)	−20.5
W7	1.77	113	218	150	317	346	01(P33)	P33	05'(P33)	−23.3
W8	1.70	170	334	168	166	359	02(P33)	P33	05'(P33)	−24.6
W9	1.72	108	95	146	2	10	01(P34)	P34	05'(P34)	−33.4
W10	1.61	121	203	150	318	358	01(P34)	P34	05'(P34)	−25.1
W11	1.72	116	159	176	333	269	02(P34)	P34	05'(P34)	−26.8
W12	1.80	118	18	163	6	17	02(P34)	P34	05'(P34)	−18.5
W13	1.54	136	337	159	33	53	01(P35)	P35	05'(P35)	−24.8
W14	1.88	106	263	135	271	353	01(P35)	P35	05'(P35)	−18.9
W16	1.87	101	122	146	359	358	01(P36)	P36	05'(P36)	−24.0
W17	1.65	110	290	147	298	358	01(P36)	P36	05'(P36)	−19.7
W18	1.97	113	208	150	319	346	01(P36)	P36	05'(P36)	−16.8
W19	1.84	120	120	129	9	379	01(P37)	P37	05'(P37)	−16.2
W21	1.73	119	208	154	325	511	01(P37)	P37	05'(P37)	−12.8
W22	1.81	99	180	180	330	347	02(P37)	P37	05'(P37)	−3.7
W23	2.15	131	126	197	10	324	02(P37)	P37	05'(P37)	−37.0
W24	1.80	102	48	148	9	17	01(P38)	P38	05'(P38)	−17.9
W25	1.73	100	287	158	303	315	01(P38)	P38	05'(P38)	−22.2
W26	1.73	106	216	174	318	338	01(P38)	P38	05'(P38)	−16.7
W27	1.69	123	327	155	316	154	02(P38)	P38	05'(P38)	−9.4
W29	1.91	147	80	136	36	356	O2'(S33)	C2'(S33)	C3'(S33)	−15.6
W30	1.64	140	107	123	0	357	O2(U33)	C2(U33)	N1(U33)	−9.3
W31	1.99	179	348	146	53	319	O4(U33)	C4(U33)	C5(U33)	−9.6
W32	1.91	129	357	142	1	353	O6(G34)	C6(G34)	C5(G34)	−13.9
W33	1.88	121	6	147	11	174	N3(G34)	C2(G34)	N2(G34)	−12.8
W34	1.77	153	42	161	336	164	O6(G34)	C6(G34)	N1(G34)	−9.9
W35	2.68	142	35	36	266	219	N2H2(G34)	N2(G34)	C2(G34)	−8.3
W36	1.90	125	9	179	331	355	N3(A35)	C4(A35)	N9(A35)	−10.9
W37	1.88	123	3	158	67	271	N1(A35)	C6(A35)	N6(A35)	−9.7
W39	1.83	118	183	168	5	41	N1(A36)	C6(A36)	C5(A36)	−5.2
W40	2.14	158	3	168	184	123	O6(Y37)	C6(Y37)	C5(Y37)	−8.7
W41	2.00	103	40	180	154	5	N7(Y37)	C5(Y37)	C6(Y37)	−9.5

site of P37 group induces the confrmation of phosphodiester (phosphodiester torsion angles–ω'_{36}, ω_{37}) to tg^- conformation which is appropriate for loop and bends. Thus tg^- conformation makes the large Y37 flexible so that the Y base is so satisfied sterochemically when *t*RNA interacts with *m*RNA.

The Effects of Mg^{2+} on the Hydration

The optimum locations and binding energies of 37 water molecules attached to the anticodon loop of yeast $tRNA^{phe}$ are listed in Table 5. The weakly bound water molecules belonging to the first hydration shell were not considered. These water molecules were compared with those[9] which had been obtained without considering Mg^{2+}.

Hydration of Phosphates. 25 water molecules are bound to anionic oxygens of seven phosphate groups with the average binding energy of −20.8 kcal/mole. W20 and W15 bound to P35 when there was no Mg^{2+}, were removed because of the repulsion of W19 and W14, respectively. In Figure 3, one sees the projection onto the plane of base 35 of the anticodon loop indicating the locations of water molecules attached to mainly phosphates.

Hydration of Sugars and Bases. 12 water molecules are bound to sugars and bases of the anticodon loop with the average binding energy of −10.9 kcal/mole. Instead of W32, which had the strongest binding energy when there was no Mg^{2+}, W29 with the binding energy of −15.6 kcal/mole was found to be the most favorable hydration site. W35 and W39 which are bound to anticodon, are bound much weakly, and removed more easily when the base-pairing between the anticodon triplet and its corresponding codon occurs during the protein synthesis.

Comparison. In Table 6, when distances between$[Mg(H_2O)_5]^{2+}$ and other water molecules are shorter than 4 Å, the repulsion between other water molecules and five bound

TABLE 6: Mg^{2+} Effect on the Hydration (kcal/mole)

	–	Mg^{2+}
Binding energy(P)	−20.4	−20.8
Binding energy(B)	−12.5	−10.9
$d(Mg^{2+}-H_2O)$	4Å>d	Increase
	10Å<d	Decrease

$Mg^{2+}(-1065)>43\ H_2O(-600)$

TABLE 7: Group Interaction (kcal/mole)

	37P–Other P groups	37P–Other S groups	37Y–Other P groups
I. Hydrated state	304	−147	−254
II. bound Mg^{2+} and hydrated state	−179	55	−585
ΔE(II–I)	−483	202	−331

Nonhydrated : −53, hydrated: −254, bound Mg^{2+} and hydrated: −752.

water molecules in $[Mg(H_2O)_5]^{2+}$ are larger than the attraction between other water molecules and five bound water molecules in $[Mg(H_2O)_5]^{2+}$. Thus the binding energies of water molecules decrease and distances between water molecule and $[Mg(H_2O)_5]^{2+}$ are larger. When distance between $[Mg(H_2O)_5]^{2+}$ and other water molecules are longer than 10 Å, the attraction between water molecule and Mg^{2+} in $[Mg(H_2O)_5]^{2+}$ are larger than the repulsion between water molecule and five bound water molecules in $[Mg(H_2O)_5]^{2+}$. Thus the binding energies of water molecules increase and the distances between water molecule and $[Mg(H_2O)_5]^{2+}$ are shorter.

And the interaction energy with Mg^{2+} and the model compound is −1,065 kcal/mole which is larger than that with 42 water molecules in the first hydration shell and anticodon loop (600 kcal/mole). Hence, Mg^{2+} much stabilizes the model compound than the water molecules in the first hydration shell of the anticodon loop.

The Stabilization of the Anticodon Loop due to Mg^{2+} and the Hydration.

In this calculation, Mg^{+2} was considered to be attached to the anionic oxygen of P37 group. In Table 7, it is seen that the total interaction energy between the 21 different groups in their $[Mg(H_2O)_5]^{2+}$ bound state is −757 kcal/mole compared to −245.4 kcal/mole in their $[Mg(H_2O)_5]^{2+}$ non-bound state. The stabilization energy due to the $[Mg(H_2O)_5]^{2+}$ binding to the anticodon loop is thus of the order of 500 kcal/mole.

The increase of attraction between P37 and other phosphate groups because of the negative charge distribution of the may O's of other P groups is the major contribution to the stabilization due to the binding of $[Mg(H_2O)_5]^{2+}$, and when it is compared with the only hydrated state, this effect amounts to about −483 kcal/mole. But the binding of $[Mg(H_2O)_5]^{2+}$ gives rise to the decrease of the attractive interactions between P37 and other sugar groups because of the positive charge distribution of the many C's of the sugar group, and this effect amounts to about +202 kcal/mole. $[Mg(H_2O)_5]^{2+}$ also produces the increase or decrease on the interaction energies between the P37 and other base groups according to the charge distribution of the bases.

And the group interaction energies between Y37 and other phosphate groups much increase because the water molecule bound to the Mg^{2+} and hydrogen bonded to the N7 of Y37 and water molecules bound to Y37 are located at the central site of the anticodon loop, and this effect amounts to about −331 kcal/mole.

Conclusion

The main results drawn from this work are as follows.

(1) $[Mg(H_2O)_5]^{2+}$ located at the E site of P37 by the binding with five water molecules stabilizes the whole anticodon loop and maintains the three dimensional structure of the tRNA.

(2) $[Mg(H_2O)_5]^{2+}$ at the E site of P37 induces the conformation of the phosphodiester (ω'_{36}, ω_{37}) to t_g^- conformation which is appropriate sterochemically when the base-pairing between the anticodon triplet and its corresponding codon occurs during the protein synthesis.

(3) $[Mg(H_2O)_5]^{2+}$ stabilizes the P groups of the anticodon loop mainly by the coulombic attraction energy between $[Mg(H_2O)_5]^{2+}$ and the anionic oxygen atoms of the P groups.

(4) $[Mg(H_2O)_5]^{2+}$ pulls water molecules, which locate in longer distance than 10 Å when $[Mg(H_2O)_5]^{2+}$ is not present, by the attraction between Mg^{2+} and water molecules in the first hydration shell. On the other hand $[Mg(H_2O)_5]^{2+}$ pushes water molecules, which locate in shorter distance than 4 Å when $[Mg(H_2O)_5]^{2+}$ is not present, by the repulsion between five water molecules in $[Mg(H_2O)_5]^{2+}$ and water molecules in the first hydration shell.

Acknowledgement. This work is supported by Korea Rerearch Center for Theoretical Physics and Chemistry.

References

(1) B. Pullman, N. Gresh, H. Berthod and A. Pullman, *Theoret. Chim. Acta (Berl.)*, **44**, 151 (1977).

(2) G. J. Quigley, M. M. Teeter and A. Rich, *Proc. Natl Acad. Sci. U. S.*, **75**, 64 (1978).

(3) T. Lindahl, A. Adams and J. R. Fresco, *Biochemistry*, **55**, 941 (1966).

(4) N. T. Record, Jr., *Biopolymers*, **14**, 2137 (1975).

(5) A. Jack, J. E. Ladner, D. Rhodes, R. S. Brown and A. Klug, *J. Mol. Biol.*, **111**, 315 (1977).

(6) S. R. Holbrook, J. L. Sussman, R. W. Warrant, G. M. Church and S. H Kim. *Nucleic Acids Res.*, **4**, 2811 (1977).

(7) J. D. Robertus, J. E. Ladner, J. T. Finch, D. Rhodes, R. S. Brown, B. F. C. Clark and A. Klug, *Nature*, **250**, 546 (1974).

(8) C. Stout, J. Mizuno, J. Rubin, T. Brennan, S. Rao and M. Sundaralingam, *Nucleic Acids Res.*, **3**, 1111 (1976).

(9) K. Kim and M. S. Jhon, *Biochim. Biophys. Acta*, **565**, 131 (1979).

(10) D. Perahia, M. S. Jhon and B. Pullman, *Biochim. Biophys. Acta*, **474**, 349 (1977).

(11) J. Caillet and P. Claverie, *Acta Cryst.*, A**31**, 448 (1975).
(12) J. Caillet and P. Claverie, *Biopolymers*, **13**, 601 (1974).
(13) V. Renugopalakrishnan, A. V. Lakshminarayanan and V. Sasisekharan, *Biopolymers*. **10**, 1159 (1971).
(14) G. Del Re, *J. Chem. Soc.*, **4031**, (1958).
(15) J. S. Muirhead-Gould and K. J. Laidler, "Chemical Physics of Ionic Solutions", John Wiley and Sons, New York, N.Y., 1966.
(16) R. H. Stokes, *J. Amer. Chem. Soc.*, **86**, 979 (1964).
(17) B. Pullman, A. Pullman and H. Berthod, *Int. J. Quant. Chem., Quant. Bio. Symp.*, **5**, 79 (1978).
(18) G. J. Quigley, N. C. Seeman, A. H. J. Wang, F. L. Suddath and A. Rich, *Nucleic Acids Res.*, **2**, 2329 (1975).
(19) H. P. Thompson, *J. Chem. Phys.*, **47**, 3407 (1967).
(20) R. Fletcher, Fortran Subroutines for Minimization by Quasi-Newton Methods, A. I. R. E. Report R7125 (1972).

Vacuum Ultraviolet Photolysis of Ethyl Bromide at 104.8-106.7 nm

Hong Lae Kim, Hee Soo Yoo and Kyung-Hoon Jung*

Department of Chemistry, Korea Advanced Institute of Science, Seoul 131, Korea *(Received March 20, 1981)*

Vacuum ultraviolet photolysis of ethyl bromide was studied at 104.8–106.7 nm (11.4–11.6 eV) in the pressure range of 0.2–18.6 torr at 25 °C using an argon resonance lamp with and without additives, *i. e.*, NO and He. Since the ionization potential of CH_3CH_2Br is lower than the photon energy, the competitive processes between the photoionization and the photodecomposition were also investigated. The observations indicated that 50% of absorbed light leads to the former process and the rest to the latter one. In the absence of NO the principal reaction products for the latter process were found to be CH_4, C_2H_2, C_2H_4, C_2H_6, and C_3H_8. The product quantum yields of these reaction products showed two strikingly different phenomena with an increase in reactant pressure. The major products, C_2H_4, and C_2H_6, showed positive effects with pressure whereas the effects on minor products were negative in both cases, *i.e.*, He and reactant pressures. Addition of NO completely suppresses the formation of all products except C_2H_4 and reduces the C_2H_4 quantum yield. These observations are interpreted in view of existence of two different electronically excited states. The initial formation of short-lived Rydberg transition state undergoes HBr molecular elimination and this state can cross over by collisional induction to a second excited state which decomposes exclusively by carbon–bromine bond fission. The estimated lifetime of the initial excited state was $\sim 4\times10^{-10}$ sec. The extinction coefficient for CH_3CH_2Br at 104.8–106.7 nm and 25 °C was determined to be $\varepsilon=(1/PL)\ln(I_0/I_t)=2061\pm160$ atm^{-1}cm^{-1} with 95% confidence level.

Introduction

In this study 104.8–106.7 nm photolysis of ethyl bromide was carried out in the pressure range 0.2–20 torr. Previous studies have shown that the modes of primary photochemical decomposition are wavelength dependent.[1]

In the ultraviolet region electronic transitions of haloalkanes are termed $n\rightarrow\sigma^*$ and their broad maximum appears at about 250 nm[2] and the short wavelength side of this absorption frequently extends into the vacuum ultraviolet region where it may overlap the far more intense absorption associated with Rydberg type transitions. Therefore, it is quite probable that in certain cases the primary products of photodecomposition differ in two regions of the spectrum. For example, Fujimoto and Wijnen[3] have investigated the photolysis of CD_3CHCl_2 where at greater than 220 nm the carbon-halogen bond fission is a predominant primary photodecomposition process, while Cremieux and Herman[4] reported that the major primary process of photodecomposition of CH_3CH_2Cl at 123.6 nm was molecular elimination of HCl.

Tschuikow-Roux and co-workers have investigated the photolyses of CH_3CH_2F,[5] CH_3CH_2Cl,[6] and other fluoroethyl chlorides[7–10] at 147 nm and 123.6 nm. They reported the major primary process as molecular elimination and in the shorter wavelength photolysis the portion of molecular elimination increased. So they suggested that carbon-halogen bone fission should be associated with the first ($n\rightarrow\sigma^*$) absorption band of the species in question, while molecular elimination processes are more clearly associated with the higher "Rydberg type" transitions, for example, $n\rightarrow4s$. The excited precursor formed at 147 nm may be sufficiently long-lived to undergo collisional modification, as the primary process is pressure dependent while that of 123.6 nm photolysis is not.

Cremieux and Herman[4] reported the photolysis of CH_3CH_2Cl at 104.8–106.7 nm using an argon resonance lamp. They reported 40 % ionization because the photon energy is above the ionization potential of CH_3CH_2Cl, and fragmentation and molecular elimination as primary processes.

Serveral workers[11–13] have investigated the photolysis of CH_3CH_2Br at greater than 200 nm where the carbon-bromine bond fission is the major primary process,